Predicting perceptual errors before stimulus onset from multimodal EEG-fNIRS functional networks

Vladimir Antipov
Research Institute of Applied Artificial Intelligence and Digital Solutions
Plekhanov Russian University of Economics
Moscow, Russia
Immanuel Kant Baltic Federal University
Kaliningrad, Russia
vantipovm@gmail.com

Vadim Grubov
Immanuel Kant Baltic Federal University
Kaliningrad, Russia
Research Institute of Applied Artificial Intelligence and Digital Solutions
Plekhanov Russian University of Economics
Moscow, Russia
vvgrubov@gmail.com

Anastasia Badarina
Research Institute of Applied Artificial Intelligence and Digital Solutions
Plekhanov Russian University of Economics
Moscow, Russia
Immanuel Kant Baltic Federal University
Kaliningrad, Russia

2026 10th Scientific School Dynamics of Complex Networks and their Applications (DCNA) | 979-8-3195-2599-4/26/$31.00 ©2026 IEEE | DOI: 10.1109/DCNA72004.2026.11733388

***Abstract*—This study examines whether the outcome of processing an ambiguous sensory stimulus can be predicted from brain functional connectivity before the stimulus is presented. Multimodal recordings from 33 participants solving Raven's Progressive Matrices were used to reconstruct a multilayer functional network for each trial. Electroencephalography source connectivity, functional near-infrared spectroscopy connectivity and cross-modal coupling between the two modalities were assembled by block composition into a single matrix, with cross-modal edges restricted to channel pairs from the same anatomical zone. Network-Based Statistic analysis localized a cluster of edges differing between correct and incorrect responses, and graph features were extracted from the induced subgraph of every trial. Feature selection by permutation importance retained the integral strength of connectivity and the mean weighted clustering coefficient as the most informative characteristics. Applied to the current trial, these features classified the response with ROC-AUC of 0.787. Applied to the preceding trial, they predicted the outcome of the next one with ROC-AUC of 0.713 and recall of 0.721 for incorrect responses. These results indicate that the current functional state of the brain, described by multimodal connectivity, carries information about the readiness of the cognitive system to process an upcoming stimulus.**

***Index Terms*—multimodal functional connectivity, EEG, fNIRS, multilayer network, Network-Based Statistic, error prediction, Raven's Progressive Matrices, Random Forest**

I. Introduction

Perception of ambiguous sensory information relies on coordinated activity of spatially distributed cortical areas that form functional networks [1], [2]. When a stimulus admits several interpretations, the outcome of perception is determined not only by the stimulus itself, but also by the functional state of the brain at the moment of its presentation [3]. Solving Raven's Progressive Matrices is a representative example of such a task, since ambiguity here arises both at the perceptual level and during the analysis of spatial and logical relations, and requires the integration of attention, working memory and executive control [4]–[7].

The work was supported by the Russian Science Foundation (Grant No. 23-72-10016-P)

Functional connectivity in these conditions is commonly assessed using a single recording modality. Electroencephalography (EEG) provides high temporal resolution and gives access to fast oscillatory interactions, whereas functional near-infrared spectroscopy (fNIRS) is sensitive to slow hemodynamic changes associated with the metabolic activity of cortical areas [8]–[10]. Analyzing each modality separately does not account for the consistency between electrical and hemodynamic processes, which limits the interpretation of cognitive processes evolving on different time scales [11]. A joint description of both modalities can be obtained within a multilayer network, where the layers correspond to intramodal interactions and the interlayer links describe cross-modal coupling [12], [13].

Network characteristics estimated during stimulus processing carry information about the outcome of the current trial and can be used for its classification [14], [15]. At the same time, the state of the brain preceding the stimulus also affects the efficiency of subsequent processing, and preparatory activity has been shown to be informative for predicting errors [3], [16], [17]. This makes it possible to consider the functional network reconstructed during the previous trial as an estimate of the current functional state and to use it for forecasting the outcome of the trial that follows.

In this study, we reconstruct multimodal EEG–fNIRS functional networks for individual trials of the Raven's Progressive Matrices task and extract graph features of the subnetwork that differs between correct and incorrect responses. We then evaluate whether these features, obtained from the previous trial, allow the outcome of the next trial to be predicted before the stimulus is presented.

II. Methods

A. Participants and Experimental Paradigm

The analysis was performed on multimodal recordings from 33 healthy participants who solved Raven's Progressive Matrices. The task consisted of items divided into series of

Authorized licensed use limited to: Kant Baltic Federal Univ. Downloaded on October 23,2026 at 15:22:06 UTC from IEEE Xplore. Restrictions apply.

progressively increasing difficulty, and the participant was required to identify the pattern within the matrix configuration and select the missing element from several options. Each item admits several plausible interpretations of the spatial and logical relations, which makes the stimulus material ambiguous at both the perceptual and the analytical level. For every trial, the interval from stimulus onset to response confirmation was extracted, and the response was labelled as correct or incorrect.

B. EEG Preprocessing and Source Reconstruction

EEG signals were band-pass filtered between 1 and 40 Hz and re-referenced to the common average. Artifacts related to eye movements and cardiovascular activity were removed using independent component analysis with 63 components. Ocular components were identified automatically by their correlation with the electrooculogram, and cardiovascular components by their correlation with the photoplethysmographic channel. The selected components were rejected, the cleaned signals were reconstructed and resampled to 500 Hz.

Since connectivity estimated at the sensor level is affected by volume conduction [18], the analysis was carried out in the source space. The fsaverage template was used as the anatomical model, the source space was defined on the cortical surface with oct-6 recursive subdivision, and the forward problem was solved using a three-layer boundary element model. The noise covariance matrix was estimated from the fixation cross epochs preceding stimulus presentation. The inverse problem was solved with dynamic statistical parametric mapping (dSPM), and the distributed sources were mapped onto the 68 cortical regions of the Desikan-Killiany parcellation. For each trial, the mean time course was extracted within every region over the whole stimulus interval.

C. Intramodal Functional Connectivity

Connectivity between cortical regions was estimated by orthogonalized envelope correlation [19], which suppresses spurious correlations caused by instantaneous field spread. The source time courses were filtered in the theta (4–8 Hz), alpha (8–13 Hz) and beta (13–30 Hz) bands, and the amplitude envelope $A_i^{(b)}(t)$ was obtained from the analytic signal using the Hilbert transform [20]. For a pair of sources (i, j) and a frequency band b, the connectivity was computed as

$$E_{ij}^{(b)} = \operatorname{corr}\left(A_i^{(b)},\, A_{j\perp i}^{(b)}\right), \tag{1}$$

where $A_{j\perp i}^{(b)}$ is the envelope of the signal j orthogonalized with respect to the signal i.

The fNIRS signals were filtered with a fourth-order Butterworth band-pass filter between 0.01 and 0.4 Hz to preserve slow hemodynamic oscillations and to suppress physiological noise [21]. Connectivity was estimated separately for oxygenated (HbO) and deoxygenated (HbR) hemoglobin as the Spearman rank correlation coefficient between all channel pairs, and non-significant connections ($p > 0.05$) were set to zero. This yielded matrices $H^{(c)}$ of size 39×39 for each trial and each chromophore.

D. Cross-Modal Connectivity

The two modalities differ in their characteristic time scales and sampling rates, so the fNIRS signals were interpolated to the length of the EEG envelopes before comparison. Cross-modal connectivity was estimated as the Pearson correlation coefficient between the amplitude envelope of an EEG source and the interpolated fNIRS signal. Each cortical region and each fNIRS channel was assigned to one of four anatomical zones, frontal, temporal, parietal or occipital, and correlations were computed only within a zone, while pairs from different zones were set to zero. This restriction reflects the fact that fNIRS registers the signal from superficial cortical areas, so pairing it with spatially distant EEG sources has no neurophysiological justification.

E. Multimodal Connectivity Matrix

Cortical regions not assigned to any of the four zones, such as the cingulate and insular cortex, were excluded, leaving 58 EEG sources. For every trial t, frequency band b and chromophore c, the intramodal and cross-modal blocks were combined into a single symmetric matrix $M_t^{(b,c)}$ of size 97×97 (Figure 1). Such a matrix can be treated as a multilayer functional network in which the layers describe intramodal interactions and the interlayer links describe the coupling between electrical and hemodynamic activity [22].

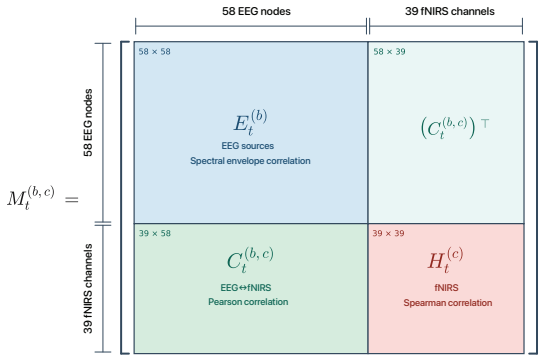


Fig. 1. Structure of the multimodal functional connectivity matrix $M_t^{(b,c)}$ formed for each trial t, EEG frequency band $b \in \{\theta, \alpha, \beta\}$ and fNIRS chromophore $c \in \{HbO, HbR\}$. The diagonal blocks $E_t^{(b)}$ and $H_t^{(c)}$ contain the intramodal connectivity between 58 EEG sources and 39 fNIRS channels, the off-diagonal blocks contain the cross-modal connectivity $C_t^{(b,c)}$ and its transposed copy.

F. Identification of the Informative Subnetwork

Before the statistical comparison, the matrix entries were converted to the Fisher z scale by taking the inverse hyperbolic tangent of the absolute correlation value, which allows correct averaging and makes the analysis sensitive to the strength of a connection irrespective of its sign. The transformed values were averaged separately over correct and incorrect trials within each participant, and the resulting matrices were symmetrized.

Differences between the two conditions were localized with the Network-Based Statistic [3], [23]. A paired t-statistic was

Authorized licensed use limited to: Kant Baltic Federal Univ. Downloaded on October 23,2026 at 15:22:06 UTC from IEEE Xplore. Restrictions apply.

computed for every edge, the suprathreshold edges formed a graph, and the size of its connected components was tested with permutation testing over 1000 iterations. Cross-modal edges connecting different anatomical zones were excluded when forming this graph, since by construction they carry zero connectivity and could produce spurious differences. A binary mask of the significant cluster was then used to extract the induced subgraph from the connectivity matrix of every individual trial.

G. Graph Features and Feature Selection

For each trial, 16 features were computed on the induced subgraph. They included the characteristics of the edge weight distribution, namely the mean absolute correlation, its standard deviation, the mean signed correlation, its standard deviation, the sum of absolute values and the proportion of positive links, the structural parameters of the subgraph, namely the number of edges, the number of active nodes, the number of connected components and the density, and the topological metrics, namely the transitivity, the mean weighted clustering coefficient, the global efficiency, the degree assortativity, the spectral radius and the algebraic connectivity. Topological characteristics were computed on the subgraph containing only the nodes incident to at least one edge of the cluster mask.

The informativeness of the features was assessed with a Random Forest classifier with class balancing under a leave-one-subject-out (LOSO) cross-validation scheme, which excludes information leakage between participants. The contribution of an individual feature was quantified by permutation importance: the values of the feature in the test fold were shuffled, the decrease in ROC-AUC with respect to the original prediction was measured, and the procedure was repeated 10 times for every feature and averaged over folds. Features with a positive contribution were retained for the predictive model.

H. Prediction of the Next Trial Outcome

To forecast the outcome before stimulus presentation, pairs of consecutive trials were formed, in which the response to the current trial $t+1$ was predicted from the graph features extracted from the preceding trial t. Only pairs with consecutive trial numbers were included, which preserved the continuity of the cognitive process. Classification was performed with a Random Forest with class balancing, missing values were imputed with the median and the features were standardized. Hyperparameters were tuned by randomized search with 50 iterations, with the number of trees varied from 100 to 600, the maximum depth from 3 to 15, the minimum number of samples per leaf from 2 to 20 and the fraction of features considered at a split from 0.3 to 1.0. The quality criterion in the search and in the final evaluation was the ROC-AUC obtained under the LOSO scheme.

III. Results

NBS analysis comparing multimodal networks between correct and incorrect responses identified a statistically significant cluster of edges, which included EEG–EEG, fNIRS–fNIRS and cross-modal EEG–fNIRS connections. This cluster was used as a mask to extract the induced subgraph from the connectivity matrix of each individual trial.

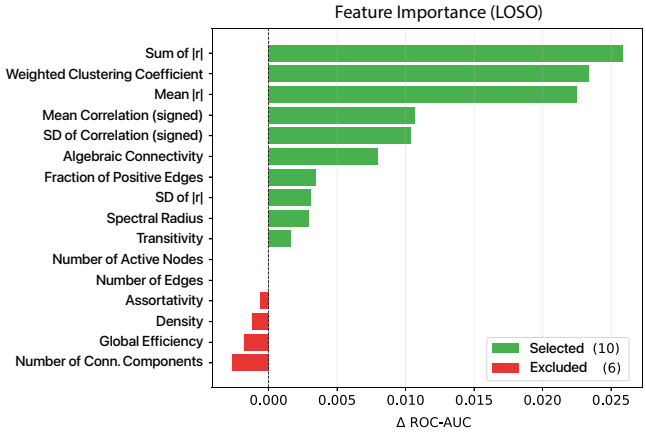


Fig. 2. Permutation importance of the graph features of the NBS cluster for the classification of correct and incorrect responses. The horizontal axis shows the mean decrease in ROC-AUC after shuffling the values of a feature, averaged over the folds of the LOSO validation. Green denotes the features retained for further analysis (positive importance, 10 features), red denotes the features excluded from the model (zero or negative importance, 6 features). Here r is the correlation coefficient between a pair of network nodes and SD is the standard deviation.

Out of the 16 graph features computed on this subgraph, 10 showed a positive contribution to classification quality (Figure 2). Highest informativeness was obtained for the characteristics of the edge weight distribution, namely the sum of absolute correlations (ΔROC-AUC $= 0.026$) and the mean absolute correlation (0.023), together with the topological metric of the mean weighted clustering coefficient (0.023). A second group was formed by the mean signed correlation and its standard deviation (about 0.010 each) and by the algebraic connectivity (0.008), while the proportion of positive links, the standard deviation of the absolute correlation, the spectral radius and the transitivity contributed from 0.002 to 0.003. Six features were excluded: the number of active nodes and the number of edges are constant for a fixed cluster mask, whereas degree assortativity, density, global efficiency and the number of connected components produced a negative permutation importance and therefore introduced noise into the model.

Such a composition of the informative set indicates that differences between correct and incorrect performance are determined by the integral characteristics of the edge weight distribution and by the topological organization of the subgraph rather than by its size or density. Dominance of the features reflecting the overall strength of connectivity suggests that successful performance is associated with the general level of coordinated activity between the network nodes, while the high informativeness of the mean weighted clustering coefficient points to the role of local integration between functionally close areas [24].

Using the current trial data, these 10 features allowed the outcome to be classified with ROC-AUC $= 0.787$ for the Random Forest model and 0.765 for SVM with a radial basis

Authorized licensed use limited to: Kant Baltic Federal Univ. Downloaded on October 23,2026 at 15:22:06 UTC from IEEE Xplore. Restrictions apply.

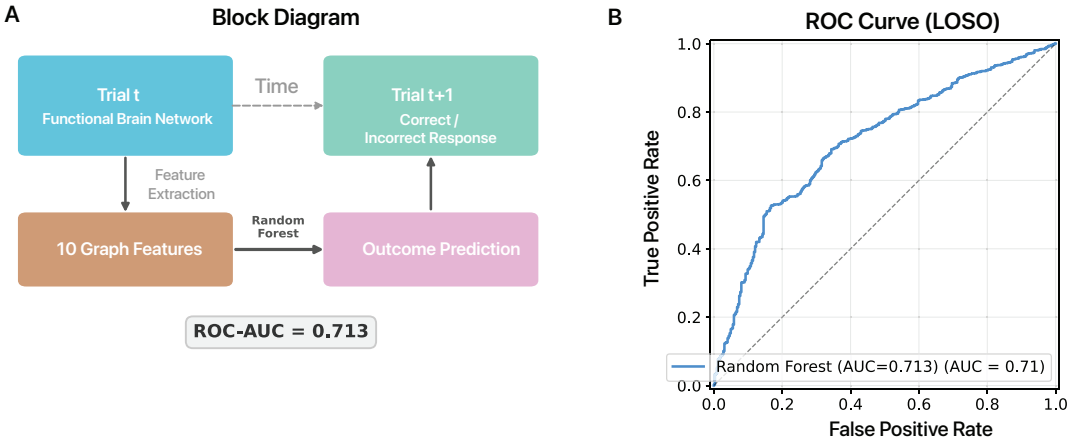


Fig. 3. Prediction of errors in sensory information processing before stimulus presentation. (A) Block diagram of the approach: the outcome of the current trial $(t+1)$ is predicted from the characteristics of the multimodal functional network estimated from the data of the previous trial (t) using a Random Forest model. (B) ROC curve of the model with the area under the curve AUC $= 0.71$. Evaluation was performed under the leave-one-subject-out scheme.

kernel. Shifting the analysis to the pre-stimulus regime, in which the features of the previous trial t were used to predict the response in the trial $t+1$, the model reached ROC-AUC $= 0.713$, which is well above the level of a random classifier (Figure 3). Accuracy was 0.609 (0.607 ± 0.105 across folds) and the weighted F1-score was 0.658. Formal accuracy lies below the baseline of 0.832 corresponding to constant prediction of the majority class, which is caused by the pronounced class imbalance, whereas ROC-AUC does not depend on the classification threshold and confirms that the model carries predictive information. Recall for the class of incorrect responses reached 0.721, so more than 72% of the cases preceding an error were identified correctly.

Decrease in classification quality with respect to the model operating on the current trial (0.713 against 0.787) is expected and reflects the incompleteness of the information available before stimulation, since the features estimated during the previous trial describe the residual state of the brain, while the actual outcome of perception also depends on fluctuations of neural activity at the moment of stimulus presentation. Stable performance above chance level and high recall for incorrect responses indicate that the current functional state of the brain contains substantial information about the readiness of the cognitive system to process an upcoming stimulus, in agreement with the influence of pre-stimulus activity on the efficiency of subsequent cognitive processing [3], [16].

Conclusion

This study shows that functional connectivity estimated jointly from EEG and fNIRS carries information about the outcome of processing ambiguous sensory stimuli, and that this information is available before the stimulus is presented. Block assembly of intramodal and cross-modal connectivity into a single matrix yields a multilayer network in which fast oscillatory and slow hemodynamic interactions are described within one formal structure, and the anatomical restriction imposed on cross-modal edges keeps this structure biologically interpretable. Comparison of correct and incorrect responses with NBS localized a cluster of edges whose graph characteristics separate the two conditions, with the strongest contribution coming from the integral strength of connectivity and the mean weighted clustering coefficient rather than from the size or density of the subgraph. Features extracted from the previous trial predicted the outcome of the next one with ROC-AUC $= 0.713$ and recall of 0.721 for incorrect responses, which is lower than for the model operating on the current trial but remains well above chance level. These findings indicate that the current functional state of the brain reflects the readiness of the cognitive system to process an upcoming stimulus and can serve as a basis for real-time monitoring of cognitive readiness and for neuroadaptive systems that support learning [25], [26].

References

[1] H. R. Heekeren, S. Marrett, P. A. Bandettini, and L. G. Ungerleider, "A general mechanism for perceptual decision-making in the human brain," *Nature*, vol. 431, no. 7010, pp. 859–862, 2004.

[2] V. Antipov, "Dynamics of oculomotor patterns during prolonged visual processing," *The European Physical Journal Special Topics*, pp. 1–8, 2025.

[3] Y.-h. Wu, E. Podvalny, M. Levinson, and B. J. He, "Network mechanisms of ongoing brain activity's influence on conscious visual perception," *Nature communications*, vol. 15, no. 1, p. 5720, 2024.

[4] T. R. Hayes, A. A. Petrov, and P. B. Sederberg, "A novel method for analyzing sequential eye movements reveals strategic influence on raven's advanced progressive matrices," *Journal of Vision*, vol. 11, no. 10, pp. 10–10, 2011.

[5] A. Badarin, V. Antipov, V. Grubov, A. Andreev, E. Pitsik, S. Kurkin, and A. Hramov, "Brain compensatory mechanisms during the prolonged cognitive task: fnirs and eye-tracking study," *IEEE Transactions on Cognitive and Developmental Systems*, 2024.

[6] V. Grubov, V. Antipov, and A. Badarin, "Brain functional connectivity in raven's progressive matrices: a fnirs study," *The European Physical Journal Special Topics*, pp. 1–9, 2026.

[7] V. A. Maksimenko, A. E. Hramov, V. V. Grubov, V. O. Nedaivozov, V. V. Makarov, and A. N. Pisarchik, "Nonlinear effect of biological feedback on brain attentional state," *Nonlinear Dynamics*, vol. 95, no. 3, pp. 1923–1939, 2019.

[8] A. E. Hramov, V. Grubov, A. Badarin, V. A. Maksimenko, and A. N. Pisarchik, "Functional near-infrared spectroscopy for the classification of motor-related brain activity on the sensor-level," *Sensors*, vol. 20, no. 8, p. 2362, 2020.

Authorized licensed use limited to: Kant Baltic Federal Univ. Downloaded on October 23,2026 at 15:22:06 UTC from IEEE Xplore. Restrictions apply.

[9] S. Kurkin, A. Badarin, V. Grubov, V. Maksimenko, and A. Hramov, "The oxygen saturation in the primary motor cortex during a single hand movement: functional near-infrared spectroscopy (fnirs) study," *The European Physical Journal Plus*, vol. 136, no. 5, p. 548, 2021.
[10] V. Antipov, A. Kuc, O. Piljugin, M. Khramova, and A. Badarin, "Age-related eeg functional connectivity during visual search in children," *The European Physical Journal Special Topics*, pp. 1–12, 2026.
[11] T. Codina, B. Blankertz, and A. v. Lühmann, "Multimodal fnirs–eeg sensor fusion: Review of data-driven methods and perspective for naturalistic brain imaging," *Imaging Neuroscience*, vol. 3, pp. IMAG–a, 2025.
[12] A. Crimi, R. Blanco, and C. Koba, "Investigating the interaction between eeg and fnirs: A multimodal network analysis of brain connectivity," 2024.
[13] A. Badarin, V. Antipov, S. Gordleeva, and V. Maksimenko, "Brain network dynamics during evidence accumulation in memory task: evidence from fnirs and drift–diffusion model," *The European Physical Journal Special Topics*, pp. 1–10, 2026.
[14] J. Cao, E. M. Garro, and Y. Zhao, "Eeg/fnirs based workload classification using functional brain connectivity and machine learning," *Sensors*, vol. 22, no. 19, p. 7623, 2022.
[15] V. Antipov, S. Kurkin, and S. Gordleeva, "Higher-order triadic interactions in the eeg sensorimotor network during motor imagery," *The European Physical Journal Special Topics*, pp. 1–9, 2026.
[16] N. Kaboodvand, H. Karimi, and B. Iravani, "Preparatory activity of anterior insula predicts conflict errors: integrating convolutional neural networks and neural mass models," *Scientific Reports*, vol. 14, no. 1, p. 16682, 2024.
[17] A. Batmanova, A. Kuc, V. Maksimenko, A. Savosenkov, N. Grigorev, S. Gordleeva, V. Kazantsev, S. Korchagin, and A. E. Hramov, "Predicting perceptual decision-making errors using EEG and machine learning," *Mathematics*, vol. 10, no. 17, p. 3153, 2022.
[18] P. Nunez and R. Srinivasan, "Electric fields of the brain: the neurophysics of eeg, 2006," 1981.
[19] J. F. Hipp, D. J. Hawellek, M. Corbetta, M. Siegel, and A. K. Engel, "Large-scale cortical correlation structure of spontaneous oscillatory activity," *Nature neuroscience*, vol. 15, no. 6, pp. 884–890, 2012.
[20] A. E. Hramov, A. A. Koronovskii, M. K. Kurovskaya, and O. I. Moskalenko, "Synchronization of spectral components and its regularities in chaotic dynamical systems," *Physical Review E*, vol. 71, no. 5, p. 056204, 2005.
[21] L. Kralj, S. Kurkin, H. Lenasi, A. Pavlov, A. Stožer, A. E. Hramov, M. Perc, and M. Gosak, "Wavelet analysis in biomedical research: A versatile tool for multiscale signal characterization and functional connectivity analysis," *Physics of Life Reviews*, vol. 59, pp. 19–47, 2026.
[22] R. Blanco, C. Koba, and A. Crimi, "Investigating the interaction between eeg and fnirs: A multimodal network analysis of brain connectivity," *Journal of Computational Science*, vol. 82, p. 102416, 2024.
[23] A. Zalesky, A. Fornito, and E. T. Bullmore, "Network-based statistic: identifying differences in brain networks," *Neuroimage*, vol. 53, no. 4, pp. 1197–1207, 2010.
[24] H. Zhang, C. Meng, X. Di, X. Wu, and B. Biswal, "Static and dynamic functional connectome reveals reconfiguration profiles of whole-brain network across cognitive states," *Network Neuroscience*, vol. 7, no. 3, pp. 1034–1050, 2023.
[25] V. V. Grubov, M. V. Khramova, S. Goman, A. A. Badarin, S. A. Kurkin, D. A. Andrikov, E. Pitsik *et al.*, "Open-loop neuroadaptive system for enhancing student's cognitive abilities in learning," *IEEE Access*, vol. 12, pp. 49 034–49 049, 2024.
[26] T. Bukina, M. Khramova, N. Smirnov, S. Kurkin, and A. Hramov, "A neuro-symbolic approach to extracurricular activity recommendation based on cognitive profiling," in *International Conference on Artificial Intelligence in Education*. Cham: Springer Nature Switzerland, 2026, pp. 309–324.

Authorized licensed use limited to: Kant Baltic Federal Univ. Downloaded on October 23,2026 at 15:22:06 UTC from IEEE Xplore. Restrictions apply.